Periodic Cycling of Plate Columns: Mass Transfer with Nonideal Liquid Draining

I. A. FURZER

Department of Chemical Engineering
University of Sydney
Sydney, 2006 Australia

Mathematical modeling of a periodically cycled plate column has been completed by using a liquid bypass model to describe nonideal liquid draining. A numerical solution over a wide range of parameters provides a closed envelope of feasible solutions. A region of this envelope encloses favorable operating values of the parameters, while the other region is unfavorable. Measurements of the parameters for nonideal liquid draining in a 600 mm diameter column fitted with sieve plates lead to predictions of only small improvements in separation performance. Modifications to the column intervals are required to move the parameters into a more favorable position in the solution envelope.

SCOPE

Plate columns can be operated with an on-off control action of the liquid and vapor streams termed periodic cycling. The cycle which is repeated in a regular way can be subdivided into a vapor flow period (VFP) and a liquid drain period (LDP). During the VFP, the vapor is fed to the column, and unsteady state mass transfer occurs on the plates. This is followed by the LDP, when the vapor flow rate is zero and liquid drains from plate to plate. The theory of periodic cycling of plate columns predicts major increases in separation over the conventional method of operation of plate columns. Smaller numbers of plates are required in a periodically cycled column for equal separations.

The magnitude of the separation improvements is highly dependent on the movement of liquid during the LDP. Liquid can effectively bypass the plate below at larger values of LDP. This can be seen by the spread in the discrete residence time distribution (DRTD) which is obtained by observing the discrete outputs from the column at various cycle counts, when an impulse of tracer is applied to plate 1 on the first cycle. The movement of the liquid away from an ideal plug flow to the plate below, to a nonideal flow to several plates below can be modeled by a simple liquid bypass model. The (2S) model has been effective in modeling the DRTD of a plate column and yields two model parameters (a) and (b). The mass transfer theory of periodic cycling of plate columns with the nonideal (2S) model operating in the LDP results in a reduced separation ability. This theory is important for a realistic modeling of the performance of plate columns operated in the periodic cycling mode.

CONCLUSIONS AND SIGNIFICANCE

The theory of periodic cycling of plate columns has been extended by the use of the (2S) model to describe the nonideal liquid movement during the LDP. A numerical solution of the set of differential equations describing the system has been obtained for a wide range of values of λ, ϵ, N_{pc}, and the model parameters (a) and (b). The solution can be expressed in terms of the ratio N_{ss}/N_{pc}, where N_{ss} is the equivalent number of plates in a steady state column operation that provides an identical separation, with a periodically cycled column containing N_{pc} plates. The computed results show there are large bounded regions where $N_{ss}/N_{pc} > 1$, and there are advantages in operating in the periodic cycling mode. The results also show bounded regions where $N_{ss}/N_{pc} < 1$, and periodic cycling is unfavorable. The maximum improvements occur when $a = 1.0$ and $b = 0.0$, corresponding to the ideal plug flow movement of liquid in the LDP. Increases in the (b) parameter lead to a decrease in the ratio N_{ss}/N_{pc}, but this decrease is relatively small provided $(a + b) \rightarrow 1$ and b is small.

A microprocessor controlled four-plate column fitted with sieve plates was used to obtain the (2S) model parameters (a) and (b) over a wide range of values of LDP. The results show an increasing (a) value from 0.39 to 0.48, while the (b) values increased from 0.04 to 0.18. These values of (a) and (b) were in a satisfactory agreement with the experimental values of $\bar{\eta}$, the mean fraction of liquid dropped from a plate during the LDP. When these values of (a) and (b) are incorporated in the mass transfer theory of periodically cycled plate columns, the range of improvements in N_{ss}/N_{pc} varied from 1.05 to 1.15, depending on the value of LDP. The (2S) model provides a rational explanation for the small values of N_{ss}/N_{pc} that have been reported in the literature. It also is significant in that it demonstrates the importance of the fluid dynamics during the LDP and shows that modified column intervals are required to increase the (a) parameter while maintaining the (b) parameter near zero.

0001-1541-79-2556-0600-$01.05.

The periodic operation of a plate column can be considered as a regular square wave control of the inlet liquid and vapor streams. If the edges of the square wave are neglected, then a period can be subdivided into a VFP and a LDP. During the VFP, the turbulent contact between liquid and vapor on a plate can be described as an ideal stage, where the time dependent liquid and vapor compositions leaving the plate are in equilibrium. Departures from this assumption lead to nonideal equilibria and the use of plate efficiencies, as described by Murphree (1925), Hausen (1953), Holland (1963), Standart (1965, 1971), Sargent and Murtagh (1969), and Krishna and Standard (1976). The equations that have been used in developing these plate efficiencies have all been based on a steady state analysis, whereas unsteady state conditions apply during the VFP. Gerster and Scull (1970) and Duffy and Furzer (1978) have experimentally measured the Murphree plate efficiency by an unsteady state method from

$$E_{mv} = \frac{h}{mVt} \ln \left\{ \frac{mx(0) - y_{in}}{mx(t) - y_{in}} \right\} \tag{1}$$

Values of E_{mv} correlated with vapor velocity and liquid holdup in a similar manner to the conventional steady state methods. These correlations can be considered as the point or local Murphree vapor efficiency as the turbulent motion on the plate enhances a well-mixed state. This contrasts with conventional plates fitted with downcomers and weirs, when the liquid cross flow over the plate leads to a transition from plug flow to dispersed flow and eventually at low Peclet numbers to a well-mixed state. The symbol (ϵ) has been used as the unsteady state plate efficiency, to differentiate it from values of E_{mv} obtained by steady state methods. The unsteady state methods based on treating a batch of well-mixed liquid can be written as

$$\epsilon = \frac{h}{mVt} \ln \left\{ \frac{mx(0) - y_{in}}{mx(t) - y_{in}} \right\} \tag{2}$$

During the LDP, liquid on a plate moves rapidly down the column and mixes with liquid on plates below. The fluid dynamics during this brief period of 1 to 2 s must account for the following:

1. The initial rapid decrease in vapor velocity and a rapid fall in froth height.
2. Partial froth collapse and the formation of a continuous liquid phase by phase inversion.
3. The flow of liquid through the orifices in the sieve plate.
4. The gravity fall of liquid and a time delay before reaching the plate below.
5. Mixing with liquid on the plate below.
6. Penetration of the liquid on the plate below and the effective liquid bypassing of this plate.
7. A continuation of 5 and 6 to further plates below depending on the length of the LDP.

We can define an ideal LDP as the movement of liquid that replaces all of the liquid holdup on a plate by the liquid holdup on the plate above. Such an ideal LDP assumes equal liquid holdups on all plates, and no mixing occurs with liquid on other plates. A partial ideal LDP can be defined as the movement of liquid that replaces a fraction (η) of the liquid holdup on a plate by the same amount of liquid from the plate above. If η is equal for all plates, then the liquid holdups must also be equal on all plates. With a partial ideal LDP, mixing occurs only between liquid on adjacent plates.

A nonideal LDP can be defined as the movement of liquid from a plate to more than one other plate in the column. It can be characterized by a spread about the mean in the DRTD and an early breakthrough in the DRTD. A spread in the DRTD can be obtained by modeling the liquid movement by a series of well-mixed stages during the LDP as described by Horn and May (1968) and Gerster and Scull (1970). Another model that can provide a spread in the DRTD is the (2S) model of Furzer and Duffy (1976) in which fractions (a) and (b) of the liquid holdup are transferred to the next two stages, respectively (see Figure 1). The advantage of the (2S) model is that it is only concerned with the liquid holdups on a plate at the start and end of the LDP. This leads to a set of algebraic equations for the n plates in the column, which can be solved to provide the liquid holdup distribution when a pseudo steady state has been reached. Another advantage of the (2S) model to account for a nonideal LDP is the ease in writing mass balances for a component. These mass balance equations provide the new initial conditions at the start of the next VFP.

LIQUID HOLDUP DISTRIBUTION

If M is the mass of liquid admitted to the column each cycle, then we can define a dimensionless holdup distribution by

$$H_n = \frac{h_n}{M} \quad n = 1, 2 \ldots N \tag{3}$$

At steady state, the mass balances for liquid on each plate can be written in the form

$$\mathbf{H} = \mathbf{A}^{-1}\mathbf{B} \tag{4}$$

where

$$\mathbf{H}^T = [H_1 \; H_2 \; . \; . \; H_N] \tag{5}$$

$$\mathbf{B}^T = [-1 \; 0 \; . \; . \; 0] \tag{6}$$

$$\mathbf{A} = \begin{bmatrix} -(a+b) & & & & \\ a & -(a+b) & & & \\ b & a & -(a+b) & & \\ & \cdot & \cdot & \cdot & \\ & & & b & a-(a+b) \end{bmatrix} \tag{7}$$

A solution is given by

$$H_1 = \frac{1}{(a+b)} \tag{8}$$

$$H_2 = \frac{a}{(a+b)^2} \tag{9}$$

$$H_n = \frac{1}{(a+b)} \{b\, H_{n-2} + a\, H_{n-1}\} \quad n = 3, 4 \ldots N \tag{10}$$

This liquid holdup distribution approaches a uniform value of $1/a$ as $b \to 0$, whereas at other values of b, the distribution has a maximum liquid holdup on plate 1, a minimum on plate 2, and intermediate values on subsequent plates down the column. It is important to note that the liquid holdup distribution is only a function of the (2S) model parameters a and b, so that $\mathbf{H} = \mathbf{H}(a, b)$.

VAPOR FLOW PERIOD

Unsteady state mass balances can be written for each plate in the column during the vapor flow period (VFP) based on the following assumptions:

1. VFP of constant length t_v.

2. Constant vapor flow rate V during VFP.
3. Well-mixed liquid on the plate during VFP.
4. The local or point Murphree vapor efficiency is constant over the plate during VFP.
5. The Murphree vapor plate efficiency is identical with the point Murphree vapor phase efficiency.
6. The column operates isothermally and contains a dilute solution, so that a linear equilibrium relationship exists, of the form $y^* = mx$.
7. Constant vapor inlet composition y_{N+1} during VFP.
8. Negligible vapor holdup.
9. Negligible entrainment or weeping.
10. Constant liquid inlet composition x_0.
11. Constant liquid holdups from cycle to cycle.

The set of equations for the unsteady state mass balances, the Murphree efficiency, and the equilibria are given by

$$h_n \frac{dx_n}{dt} = V\,(y_{n+1} - y_n) \quad n = 1, 2, \ldots N \tag{11}$$

$$\epsilon = \frac{y_n - y_{n+1}}{y^*_n - y_{n+1}} \quad n = 1, 2, \ldots N \tag{12}$$

$$y^*_n = mx_n \quad n = 1, 2, \ldots N \tag{13}$$

Elimination of y_n from these three equations results in a set of differential equations in x_n which contain an increasingly large number of terms in ϵ and powers of $(1 - \epsilon)$ as N increases. A numerical solution of this set of differential equations in x_n leads to excessive CPU times as N increases. However, retaining x_n as the independent variable leads to relatively simple expressions for the mass balances in the liquid drain period (LDP), and this method is preferred for small values of N.

Elimination of x_n from these equations leads to a simpler set of differential equations which consume a moderate amount of CPU time for their numerical solution. This method is preferred for larger values of N even though the mass balances in the LDP are more involved. The equations become

$$\frac{dy_n}{dt} = \frac{mV\epsilon}{h_n}(y_{n+1} - y_n) + (1 - \epsilon)\frac{mV\epsilon}{h_n}\frac{dy_{n+1}}{dt} \quad n = 1, 2, \ldots N \tag{14}$$

Define an average liquid and vapor flow rate over the cycle by $\overline{L} = M/t_c$ and $\overline{V} = V\,t_v/t_c$. A dimensionless parameter λ, which is the ratio of the slopes of the equilibrium and operating lines, is defined as $\lambda = m\,\overline{V}/\overline{L}$. A dimensionless time θ, defined as $\theta = t/t_v$, is used throughout the VFP. Equation (14) becomes

$$\frac{dy_n}{d\theta} = \frac{\lambda\epsilon}{H_n}(y_{n+1} - y_n) + (1 - \epsilon)\frac{\lambda\epsilon}{H_n}\frac{dy_{n+1}}{d\theta} \quad n = 1, 2, \ldots N \tag{15}$$

We can define a dimensionless vapor composition Y_n by

$$Y_n = \frac{y_n - y_{N+1}}{y^*_0 - y_{N+1}} \tag{16}$$

The term Y_n can be considered as the change in vapor composition from the inlet of the column y_{N+1} to plate n, y_n, to the maximum change across the column $(y^*_0 - y_{N+1})$. Equation (15) becomes

$$\frac{dY_n}{d\theta} = \frac{\lambda\epsilon}{H_n}(Y_{n+1} - Y_n) + (1 - \epsilon)\frac{\lambda\epsilon}{H_n}\frac{dY_{n+1}}{d\theta} \quad n = 1, 2, \ldots N \tag{17}$$

where

$$\frac{dY_{N+1}}{d\theta} = 0 \tag{18}$$

Equation (17) is in a dimensionless form suitable for solution by numerical methods. The coefficients of the terms on the right-hand side are also dimensionless and contain the dimensionless quantities λ, ϵ, and H_n. In the case of constant liquid holdups on the plate, H_n is a constant, and if both λ and ϵ are constants, then the two coefficients will retain constant values for plates numbered 1, 2, . . N. With the use of the (2S) model, the liquid holdup distribution can be calculated from Equation (4). The variation of H_n from plate to plate leads to different coefficients in Equation (17), even with constant values of λ and ϵ.

The initial conditions at the start of the first cycle when all plates are filled with liquid feed are

$$Y_n(0) = 0.0 \quad n = 1, 2, \ldots N \tag{19}$$

Integration using a variable step length method of the Runge-Kutta-Merson form is effective in numerically solving the set of differential equations with the initial condition $Y_n(0) = 0.0$ for the VFP of the first cycle. The initial conditions for subsequent cycles differ from $Y_n(0) = 0.0$ and are discussed after the liquid drain period.

We can define a dimensionless liquid composition X_n as the change in liquid composition from the liquid inlet to plate n $(x_0 - x_n)$, to the maximum change if the liquid left in equilibrium with the entering vapor:

$$X_n = \frac{x_0 - x_n}{x_0 - x^*_{N+1}} \tag{20}$$

At the end of the VFP, when $\theta = 1$, $X_n = X_n(1)$. Values of $X_n(1)$ can be calculated from expressions for the Murphree efficiency by

$$X_n(1) = 1 - \left\{ \frac{1}{\epsilon} Y_n(1) + \left(1 - \frac{1}{\epsilon}\right) Y_{n+1}(1) \right\} \quad n = 1, 2, \ldots N \tag{21}$$

LIQUID DRAIN PERIOD

At the end of the VFP, the vapor flow rate is reduced to zero, and the liquid drain period (LDP) begins. During the LDP the (2S) model allows for a fraction (a) of the plate holdup to reach the immediate plate below, and a fraction (b) reaches the second plate below. If $x_n(t_v)$ is the liquid composition on plate n at time t_v, the end of the VFP, then $x_n(0)$ the liquid composition on that plate at the end of the LDP or the start of the next cycle is given by

$$h_1 x_1(0) = h_1[1 - (a + b)]\,x_1(t_v) + M\,x_0 \tag{22}$$

$$h_2 x_2(0) = h_2[1 - (a + b)]\,x_2(t_v) + H_1\,a\,x_1(t_v) \tag{23}$$

$$h_n x_n(0) = h_n[1 - (a + b)]\,x_n(t_v) + H_{n-1}\,a\,x_{n-1}(t_v) + H_{n-2}\,b\,x_{n-2}(t_v) \quad n = 3, 4 \ldots N \tag{24}$$

If we use X_n, Equations (22) to (24) become

$$X_1(0) = [1 - (a + b)]\,X_1(1) \tag{25}$$

$$X_2(0) = [1 - (a + b)]\,X_2(1) + \frac{H_1}{H_2}\,a\,X_1(1) \tag{26}$$

$$X_n(0) = [1 - (a+b)]\, X_n(1) + \frac{H_{n-1}}{H_n} a\, X_{n-1}(1) + \frac{H_{n-2}}{H_n} b\, X_{n-2}(1) \quad n = 3, 4 \ldots N \quad (27)$$

The dimensionless composition of the liquid leaving the column X_{out} is a measure of the separating ability of the column:

$$X_{out} = H_N(a+b)\, X_N + H_{N-1}\, b\, X_{N-1} \quad (28)$$

The liquid compositions at the end of the LDP $X_1(0)$, $X_2(0)$ .. $X_N(0)$ are the new initial liquid compositions for the start of the next VFP. The new initial vapor compositions at the start of the next VFP can be calculated from the expression for the Murphree plate efficiency to give

$$Y_n(0) = \epsilon \left\{ 1 - X_n(0) - \left(1 - \frac{1}{\epsilon}\right) Y_{n+1}(0) \right\} \quad n = 1, 2, \ldots N \quad (29)$$

This initial condition differs from the original initial condition when all plates are filled with liquid feed and $Y_n(0) = 0.0$; $n = 1, 2, \ldots N$.

A computational algorithm of the numerical methods for solving the set of differential equations in the VFP and the algebraic equations in the LDP can be summarized as follows:

1. Evaluate the liquid holdup distribution in the column.
2. Set initial conditions at $Y_n(0) = 0.0$; $n = 1, 2 \ldots N$.
3. Integrate the set of differential equations in Y_n to $\theta = 1$, corresponding to the end of the VFP.
4. Evaluate the liquid composition $X_n(1)$ at the end of the VFP.
5. Evaluate the liquid compositions $X_n(0)$ at the end of the LDP or the start of the next cycle.
6. Evaluate the new initial conditions $Y_n(0)$ and restart the integration from step 3.
7. Terminate the integration when the magnitude of the error in an objective function is below some set value e.

After a sufficient number of cycles, the column approaches a pseudo steady state condition, whereby the initial conditions are repeated from cycle to cycle. We can define the time averaged vapor composition leaving plate 1 as

$$\bar{y}_1 = \frac{1}{t_v} \int_0^{t_v} y_1(t)\, dt \quad (30)$$

and

$$\bar{Y}_1 = \frac{\bar{y}_1 - y_{N+1}}{y_0^* - y_{N+1}} \quad (31)$$

or

$$\frac{d\bar{Y}_1}{d\theta} = Y_1 \quad (32)$$

Integration of Equation (32) from $\theta = 0$ to $\theta = 1$ is completed simultaneously with the numerical evaluation of the differential equation in Y_n, to yield $\bar{Y}_1(1)$. A mass balance over the column when a pseudo steady state is reached gives

$$X_{out} = \lambda \bar{Y}_1(1) \quad (33)$$

We can establish an objective function as a measure of the approach to pseudo steady state by a departure in the mass balance over the column:

$$P = 1 - \frac{\lambda \bar{Y}_1(1)}{X_{out}} \quad (34)$$

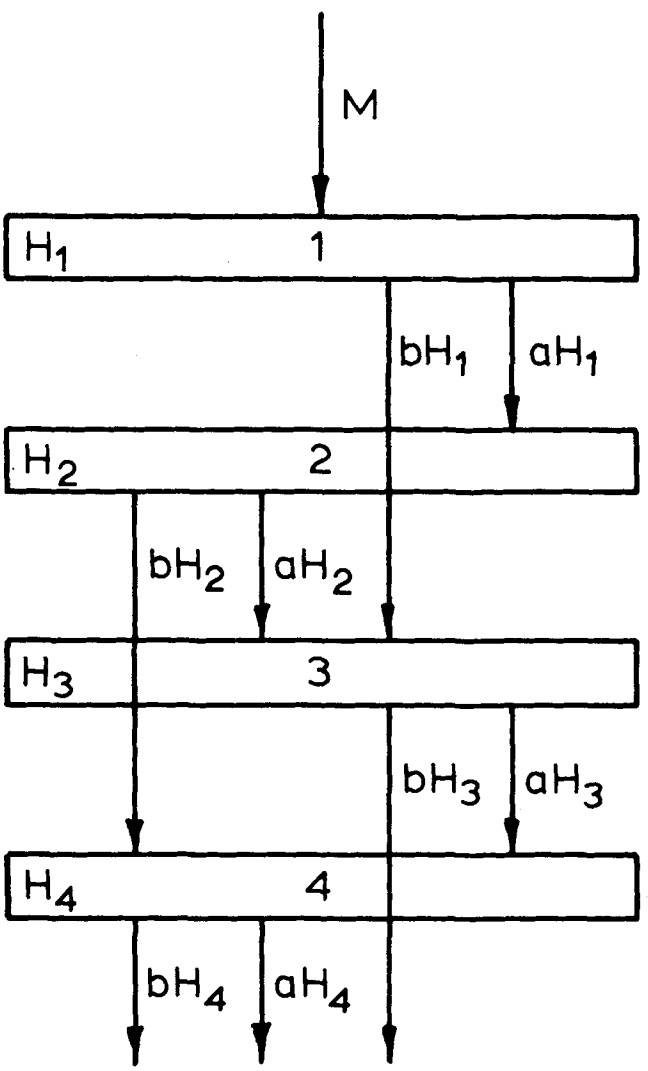

Fig. 1. Liquid movement during the LDP (2S) model.

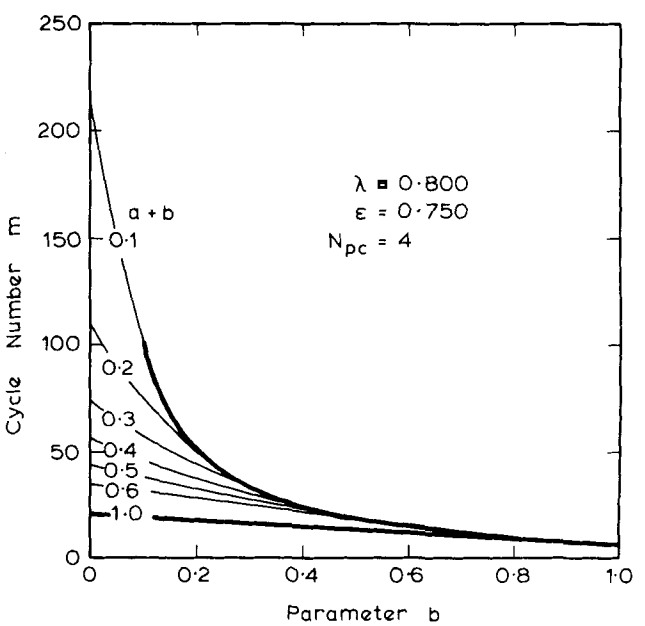

Fig. 2. Cycle number for mass balance > 99.99%.

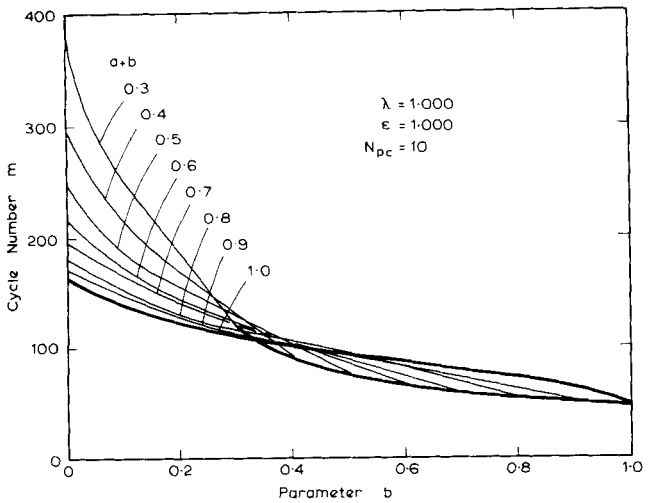

Fig. 3. Cycle number for mass balance > 99.99%.

The integration in step 7 is terminated when $P = 0.0001$ or the mass balance is satisfied to 99.99%.

SIMULATION RESULTS

A computer program written in extended FORTRAN IV was run on the CYBER computer for various values of λ, ϵ, N_{pc}, a, and b. The number of integration steps in a cycle was automatically adjusted by the program, but the number of cycles to satisfy the mass balance to 99.99% was found to be large at small values of a and b and for larger values of N_{pc}. Figure 2 shows values of the number of cycles for ranges of $(a + b)$ and b with $\lambda = 0.800$, $\epsilon = 0.750$, and $N_{pc} = 4$. This four-plate column required 220 cycles to reach a 99.99% approach to pseudo steady state when $(a + b) = 0.100$ and $b = 0.000$. This was reduced to only twenty-one cycles when $(a + b) = 1.000$ and $b = 0.000$. Even smaller numbers of cycles are obtained at larger values of b; for example, only seven cycles are required when $(a + b) = 1.000$ and $b = 1.000$. Figure 3 shows a similar figure for $\lambda = 1.000$, $\epsilon = 1.000$ and $N_{pc} = 10$. The increase in the number of plates from four to ten results in a major increase in the number of cycles to reach the pseudo steady state condition. When $(a + b) = 0.300$ and $b = 0.000$, over 379 cycles are required, while when $(a + b) = 1.000$ and $b = 0.000$, over 163 cycles are required. While the shape of the curves are more complex in Figure 3, there is a decrease in the number of cycles with increasing values of b. When $(a + b) = 1.000$ and $b = 1.000$, forty-seven cycles are still required.

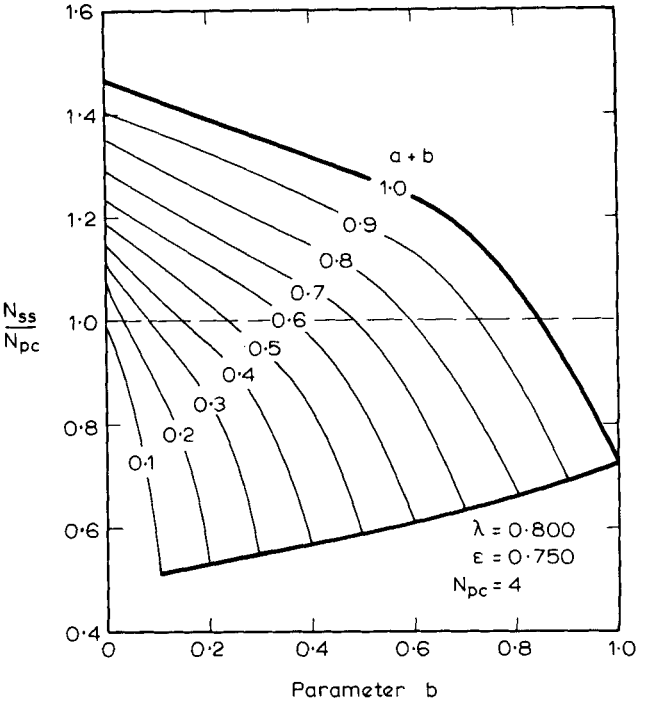

Fig. 4. Separation performance with (2S) model.

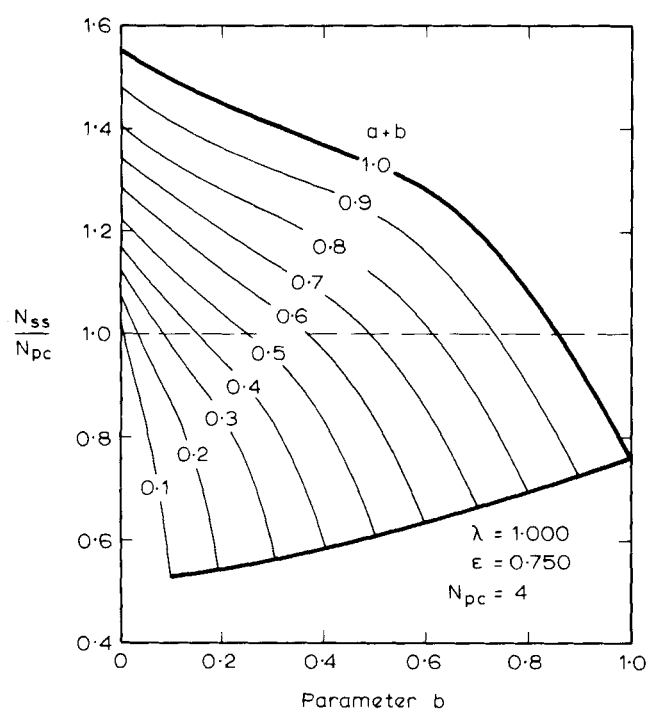

Fig. 5. Separation performance with (2S) model.

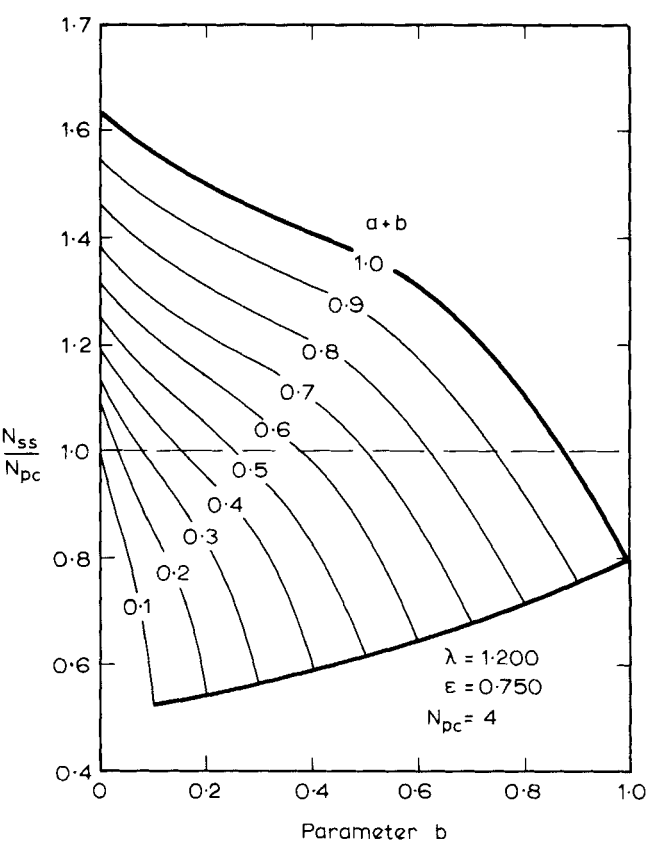

Fig. 6. Separation performance with (2S) model.

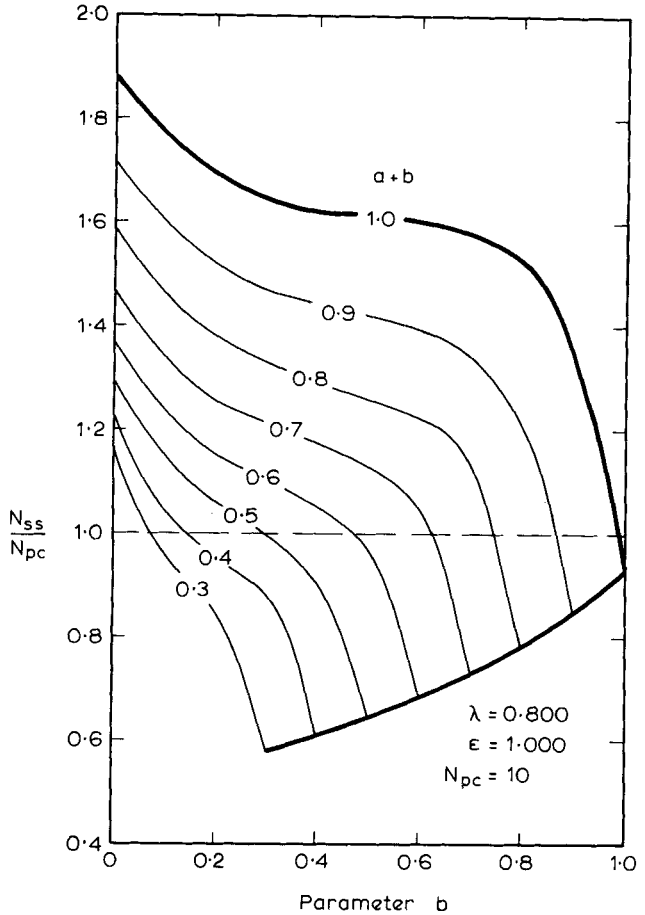

Fig. 7. Separation performance with (2S) model.

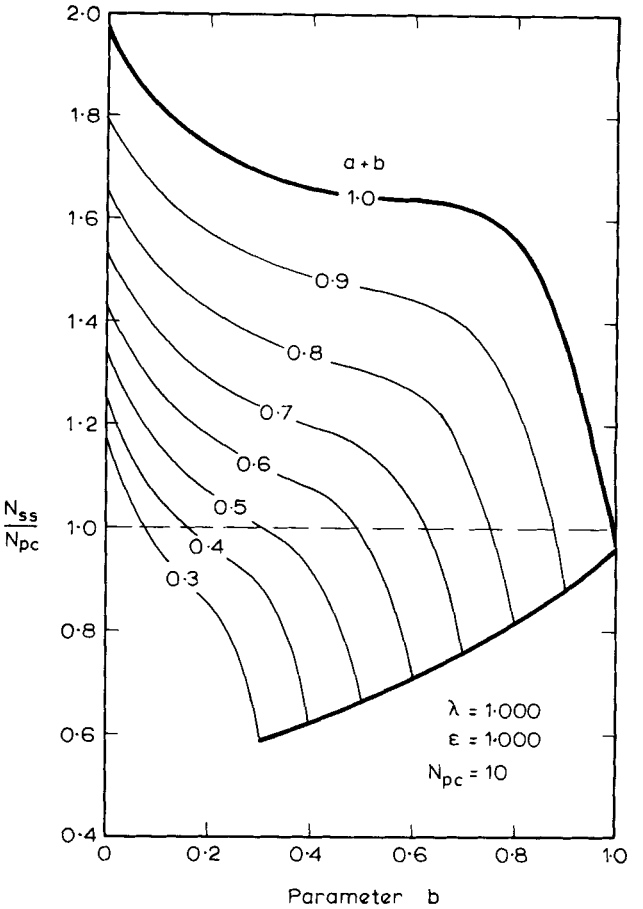

Fig. 8. Separation performance with (2S) model.

The results can be correlated by

$$m = 2.153\ N_{pc}^{1.815};\quad b = 0.000\quad 4 \leq N_{pc} \leq 10 \quad (35)$$

$$m = 2.204\ N_{pc}^{1.815};\quad b = 0.100\quad 4 \leq N_{pc} \leq 10 \quad (36)$$

Simulation of the mass transfer performance with the (2S) model was completed for a wide range of the variables λ, ϵ, a, b, and N_{pc} as shown in Figures 4 to 9. The improvements in separation in the column have been described by the term N_{ss}/N_{pc}, where N_{ss} is the number of steady state plates to provide the same separation X_{out} at identical values of λ and ϵ, and N_{pc} is the number of plates in a periodically cycled column.

Figures 4 to 9 all contain a bounded envelope which encloses feasible solutions. The upper constraint is when $(a + b) = 1.000$, while the lower constraint is when $a = 0.000$. When $(a + b) \rightarrow 0$, the number of cycles to reach a 99.99% mass balance requires excessive CPU time, and the lower constraint has been truncated at values of $(a + b) = 0.1$ and 0.3 on these figures. The bounded envelope can be subdivided into two regions about the line $N_{ss}/N_{pc} = 1.000$. Above the line, the ratio $N_{ss}/N_{pc} > 1$, and the simulation predicts improvements in the separating ability of periodically cycled columns. Below the line, the ratio $N_{ss}/N_{pc} < 1$, and the separation is unfavorable.

The effect of changes in λ from 0.800 to 1.200 is shown in Figure 4 to 6 for constant values of $\epsilon = 0.750$ and $N_{pc} = 4$. The major change is a movement towards improved separation at higher values of λ. The upper region of the bounded envelope is expanded particularly as $(a) \rightarrow 1.000$ and $(a + b) \rightarrow 1.000$. When $\lambda = 0.800$, $N_{ss}/N_{pc} = 1.475$. When $(a) = 0$ and $(a + b) = 1.000$, this ratio increases to 1.637, when $\lambda = 1.200$, Similar effects are shown on Figures 7 to 9 for constant values of $\epsilon = 1.000$ and $N_{pc} = 10$. In these cases, the upper bounded envelope is larger than the lower bounded envelope, and ratios of $N_{ss}/N_{pc} > 2$ are feasible.

Table 1 gives the computed results for a ten-plate column with $\lambda = 1.000$ and $\epsilon = 1.000$ for various values of a, b, and $(a + b)$. The number of cycles to reach 99.99% of pseudo steady state, the separation factor X_{out}, the number of theoretical plates, values of N_{ss}, and the ratio N_{ss}/N_{pc} are listed in Table 1.

DEDICATED MICROPROCESSOR SYSTEM

The equipment consisted of a perspex column 600 mm in diameter fitted with four sieve plates and controlled by a microprocessor system as shown in Figure 10. The sieve plates were of a downcomerless type and occupied the full cross-sectional area of the column. The plates were supported internally by a circumferential flange which allowed for flow visualization studies during the VFP and LDP times. The plates containing 6 mm diameter holes at 5% free area were fixed at a 600 mm plate spacing. Both the air and water flow rates could be operated in an on-off mode by the use of three-way valves. The control of these valves depended on the digital output from the microprocessor system. A stable liquid holdup distribution in the column was achieved by re-establishing the top plate holdup to a set value each cycle. The pressure drop across the top plate was measured by an electronic DP cell, and an output voltage in the range 0 to 5 V was accepted as in input to the microprocessor system.

The JOLT microprocessor system used a MOS Technology 6502, eight-bit microprocessor. Using a basic clock

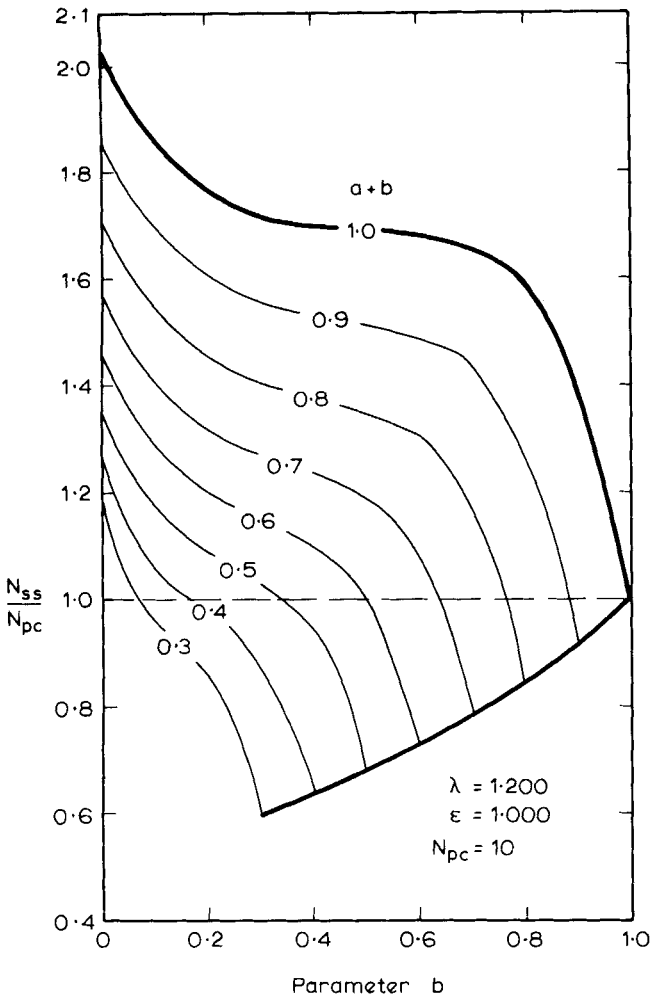

Fig. 9. Separation performance with (2S) model.

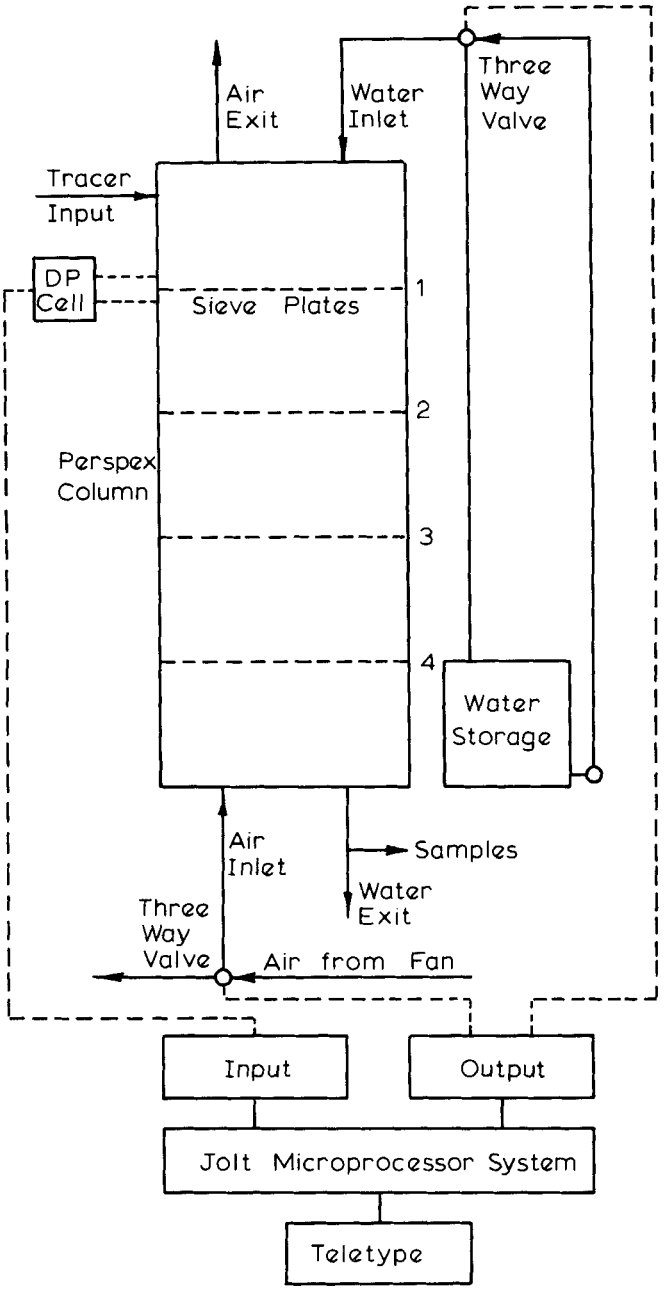

Fig. 10. Schematic diagram of column and microprocessor.

rate of 1.0 MHz, the instruction execution time was between 2 and 8 μs. A read only memory ROM contained the console microcode which enabled a teletype to be used as a control panel. The random access memory RAM contained the program for the on-off control of the column and level control of the top plate. The interface between the microprocessor and the column consists of a standard 6520 peripheral interface adaptor. Inputs to the system consisting of a real time clock and a level comparitor generate interrupts to the microprocessor. Outputs from the system pass through an additional part of the 6502 adaptor to circuitry that allows for the driving of the three-way valves in the air and water lines. The source text of the program was developed on a PDP 11/45 computer and binary tapes generated by a cross-assembler. Further details are provided by Furzer and Rosolen (1978).

Operation of the JOLT microprocessor system proved to be highly reliable and flexible. Binary programs were loaded through the teletype and stored in RAM. Execution of the program resulted in inputs of a number of parameters through the teletype. These included the time in seconds of the VFP and LDP times. The program then continued to control the column until an operator generated interrupt was passed to the program. Restarting of the program for different values of VFP and LDP was straightforward and allowed for measurements of the DRTD over wide ranges of VFP and LDP times.

A tracer consisting of a sodium chloride solution was injected onto the top plate during the VFP and acted as an impulse to the system. The output was withdrawn from below plate 4 at the end of each cycle. The tracer was analyzed by measurement of the electrical conductivity. Samples were withdrawn for a large number of cycles until the conductivity returned to the background values. This procedure was repeated for a wide range of LDP times from 0.60 to 1.80 s.

The total column holdup Σh and the mass of liquid M admitted per cycle were also measured for each run to allow for the calculation of $\bar{\eta}_{EXP}$, the mean fraction of liquid holdup dropped per cycle from

$$\bar{\eta}_{EXP} = 4M/\Sigma h$$

DISCRETE RESIDENCE TIME DISTRIBUTION

The experimental results were normalized to give the discrete residence time distribution (DRTD). Triplicate experimental measurements of the DRTD are shown on Figure 11 for a liquid drain period of 1.00 s. Duplicate measurements were obtained and the mean values of the

TABLE 1. MASS TRANSFER SEPARATIONS WITH (2S) MODEL

$\lambda = 1.000$			$e = 1.000$		$N_{pc} = 10$		
a	b	$(a+b)$	m	X_{out}	$N(e=1)$	N_{ss}	N_{ss}/N_{pc}
0.3001	0.0000	0.3001	379	0.9216	11.7474	11.7474	1.1747
0.2001	0.1000	0.3001	252	0.9058	9.6114	9.6114	0.9611
0.1001	0.2000	0.3001	185	0.8956	8.5801	8.5801	0.8580
0.0001	0.3000	0.3001	120	0.8546	5.8768	5.8768	0.5877
0.4001	0.0000	0.4001	296	0.9258	12.4713	12.4713	1.2471
0.2668	0.1333	0.4001	197	0.9111	10.2435	10.2435	1.0244
0.1334	0.2667	0.4001	145	0.9020	9.2077	9.2077	0.9208
0.0001	0.4000	0.4001	93	0.8617	6.2328	6.2328	0.6233
0.5001	0.0000	0.5001	248	0.9300	13.2876	13.2876	1.3288
0.3334	0.1667	0.5001	164	0.9164	10.9617	10.9617	1.0962
0.1668	0.3333	0.5001	121	0.9085	9.9323	9.9323	0.9932
0.0001	0.5000	0.5001	77	0.8690	6.6325	6.6325	0.6632
0.6001	0.0000	0.6001	216	0.9343	14.2143	14.2143	1.4214
0.4001	0.2000	0.6001	144	0.9218	11.7856	11.7856	1.1786
0.2001	0.4000	0.6001	106	0.9151	10.7790	10.7790	1.0779
0.0001	0.6000	0.6001	66	0.8763	7.0837	7.0837	0.7084
0.7001	0.0000	0.7001	195	0.9386	15.2763	15.2763	1.5276
0.4668	0.2333	0.7001	129	0.9272	12.7391	12.7391	1.2739
0.2334	0.4667	0.7001	96	0.9218	11.7816	11.7816	1.1782
0.0001	0.7000	0.7001	59	0.8837	7.5974	7.5974	0.7597
0.8001	0.0000	0.8001	180	0.9429	16.5048	16.5048	1.6505
0.5334	0.2667	0.8001	120	0.9327	13.8574	13.8574	1.3857
0.2668	0.5333	0.8001	90	0.9285	12.9883	12.9883	1.2988

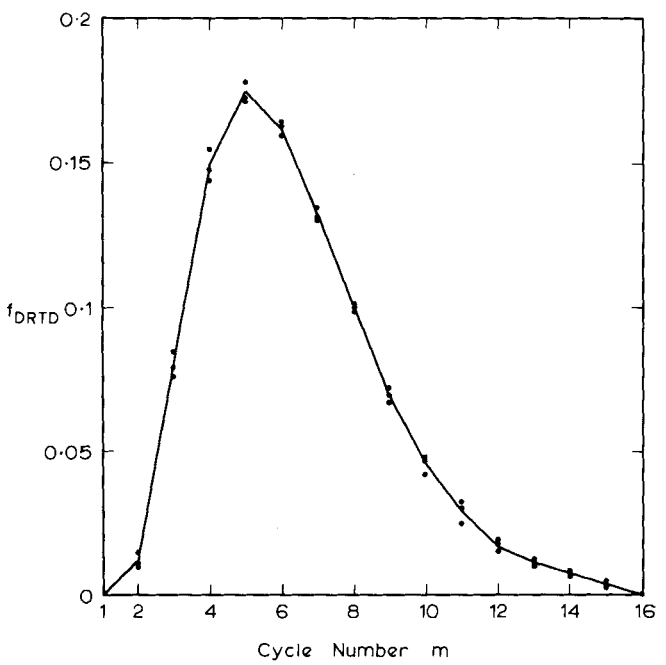

Fig. 11. DRTD measurements with LDP = 1.00 s.

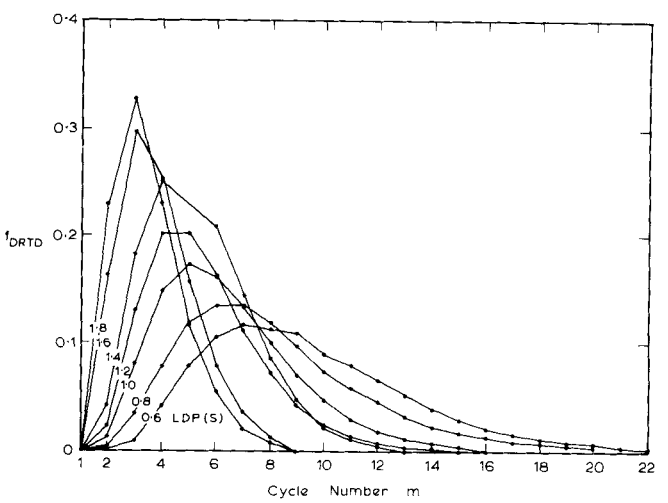

Fig. 12. DRTD measurements with LDP from 0.60 to 1.80 s.

DRTD shown on Figure 15 for values of the LDP from 0.60 to 1.80 s.

The parameters (a) and (b) in the (2S) model were obtained by an optimization program that minimized a least-squares error objective function as described by Furzer and Duffy (1976). The (2S) model is considered valid for LDP values less than 1.40 s, while higher order models of the type (3S) or (4S) are required to model the early breakthrough condition in the DRTD. For LDP in the range 0.60 to 1.40 s, values of (a) and (b) in the (2S) model that minimizes the objective function are shown on Figure 13. Values of the mean fraction of the liquid holdup $\overline{\eta}$, dropped per cycle, calculated from the (2S) model are compared with the experimental values of $\overline{\eta}_{EXP}$ on Figure 14.

DISCUSSION

The computed results for the ratio N_{ss}/N_{pc} using the nonideal (2S) model are shown on Figures 4 to 9 with the intercepts when $b = 0$ provide N_{ss}/N_{pc} ratios which are in agreement with the vector-matrix solution method of Furzer and Duffy (1974).

The measurement of the DRTD of the four-plate column, as shown on Figure 12, provides the first clear insight into the mechanism of the liquid movement through the column. Modeling of the DRTD with the (2S) model provides values of (a) ranging from 0.39 to 0.48, while (b) increases from 0.02 to 0.19, as shown on Figure 13. The rapid increase in (b) over the range of LDP from 0.60 to 1.40 s clearly indicates a considerable fraction of the plate holdup penetrating the immediate plate below and arriving at the second plate below. The experimental value of $\overline{\eta}_{EXP}$ as shown on Figure 14 when the LDP is 1.40 s is 0.77, and the (b) value is 0.19. Shown on Figure 15 are the predicted values of N_{ss}/N_{pc} for values of $(a+b)$ and (b) which were experimentally measured on the column. The ratio N_{ss}/N_{pc} ranges from 1.05 to

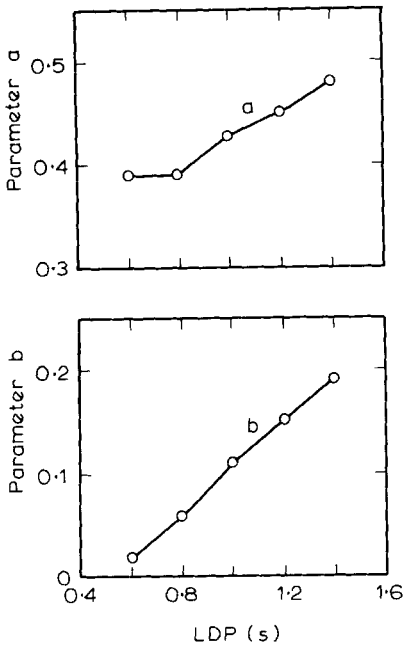

Fig. 13. Optimum values of parameters (a) and (b).

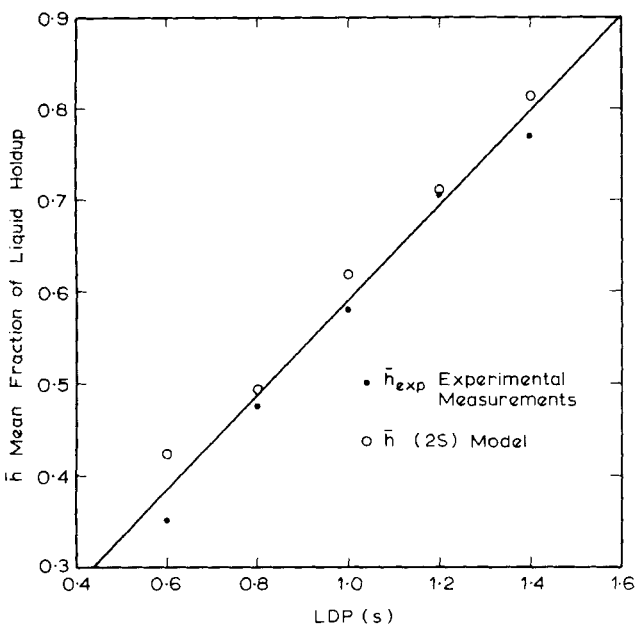

Fig. 14. Mean fraction of the liquid holdup.

1.15 with these values of (a) and (b). The maximum increase that could be expected from Figure 15, when $a = 1$ and $b = 0$, amounts to $N_{ss}/N_{pc} = 1.560$, and this is not realizable with the use of downcomerless sieve plates.

This research project demonstrates the importance of modeling the liquid movement during the LDP and the need to modify the column internals to satisfy the requirement of the parameter $(b) \rightarrow 0$. Only with these modifications can the DRTD be altered to approach an ideal LDP, when $a \rightarrow 1.0$ and the ratio N_{ss}/N_{pc} is a maximum. The use of the nonideal liquid draining model provides an insight into the results of Schrodt et al. (1967) and Gerster and Scull (1970) who were unable to obtain the high theoretical separation improvements expected in a plate column operated with periodic cycling.

ACKNOWLEDGMENT

This research project on periodic cycling is supported by the A.R.G.C. Thanks are given to W. Radford who collected the experimental data.

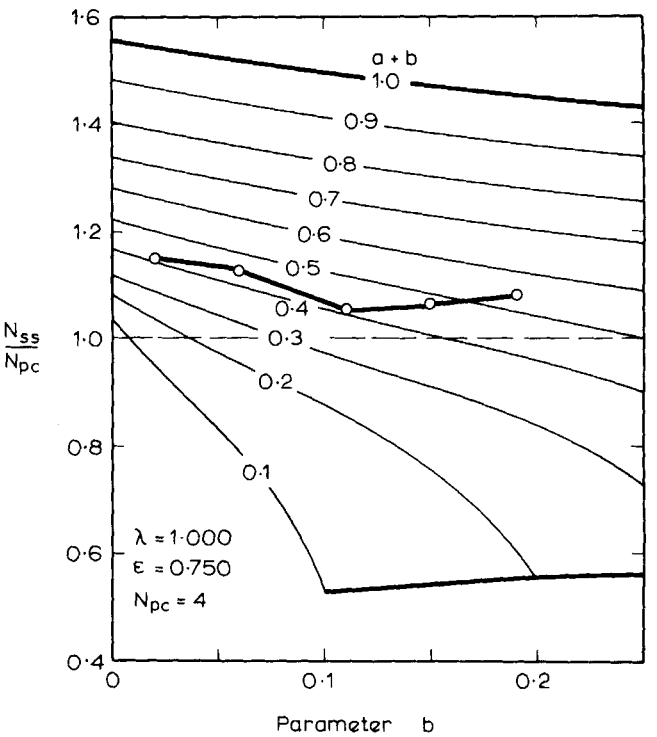

Fig. 15. Predicted separation improvements with periodic cycling.

NOTATION

a	=	parameter in the (2S) model
$\mathbf{A}$	=	matrix
b	=	parameter in the (2S) model
$\mathbf{B}$	=	column vector
E_{mv}	=	Murphree vapor plate efficiency
h	=	plate liquid holdup
H	=	dimensionless liquid holdup
n	=	plate number
N	=	number of plates in the column
m	=	slope of equilibrium line
M	=	mass of liquid admitted to the column per cycle
P	=	objective function
t	=	time
t_c, t_v	=	cycle and vapor times, respectively
V	=	vapor flow rate
x	=	liquid composition
X	=	dimensionless liquid composition
$\overline{y}_1$	=	mean vapor composition leaving plate 1
y	=	vapor composition
y^*_0	=	vapor composition in equilibrium with inlet liquid of composition x_0
$\overline{Y}_1$	=	mean dimensionless vapor composition leaving plate 1
Y	=	dimensionless vapor composition
ϵ	=	plate efficiency
η	=	fraction of liquid holdup dropped during LDP
θ	=	dimensionless time
λ	=	ratio of slopes of the equilibrium and operating lines

Subscripts

EXP	=	experimental
n	=	plate number
N	=	number of plates in the column
out	=	outlet condition
pc	=	periodic cycling
ss	=	steady state
v	=	vapor flow period

LITERATURE CITED

Duffy, G. J., and I. A. Furzer, "Mass Transfer on a Single Sieve Plate Column Operated with Periodic Cycling," *AIChE J.*, **24**, 588 (1973).

Furzer, I. A., and G. J. Duffy, "Generalized Theory of Periodically Operated Plate Columns," Joint Symposium on Distillation, University of Sydney/University of N.S.W., Australia (May, 1974).

———, "Periodic Cycling of Plate Columns: Discrete Residence Time Distribution," *AIChE J.*, **22**, No. 6, 1118 (1976).

———, "Microprocessor System for Plate Column Control," *IEEE. IECI*, **25**, No. 2, 145 (1978).

Gerster, J. A., and H. M. Scull, "Performance of Tray Columns Operated in the Cycling Mode," *AIChE J.*, **16**, 108 (1970).

Hausen, H., "Zur Definition des Austauschgrades von Rektifzierboden," *Chemie-Ingr-Tech.*, **25**, 595 (1953).

Holland, C. D., *Multicomponent Distillation*, Prentice-Hall, Englewood Cliffs, N.J. (1963).

Horn, F. J. M., and R. A. May, "Effect of Mixing on Periodic Countercurrent Processes," *Ind. Eng. Chem. Fundamentals*, **1**, 349 (1968).

Krishna, R., "A Film Model Analysis of Non-equimolar Distillation of Multicomponent Mixtures," *Chem. Eng. Sci.*, **32**, 1197 (1977).

———, and G. L. Standard, "A Multicomponent Film Model Incorporating a General Matrix Method of Solution to the Maxwell-Stefan Equations," *AIChE J.*, **22**, 383 (1976).

Murphree, E. V., "Rectifying Column Calculations," *Ind. Eng. Chem.*, **17**, 747 (1925).

Sargent, R. W. H., and B. A. Murtagh, "The Design of Plate Distillation Columns for Multicomponent Mixtures," *Trans. Inst. Chem. Engrs.*, **47**, T85 (1969).

Schrodt, V. N., J. T. Sommerfeld, O. R. Martin, P. E. Parisot, and H. H. Chien, "Plant-scale Study of Controlled Cyclic Distillation," *Chem. Eng. Sci.*, **22**, 759 (1967).

Standardt, G., "Studies in Distillation-V. Generalized Definition of a Theoretical Plate or Stage of Contacting Equipment," *ibid.*, **20**, 611 (1965).

———, "Comparison of Murphree-type Efficiencies with Vaporisation Efficiencies," *ibid.*, **26**, 985 (1971).

Manuscript received June 9, 1978; revision received January 24, and accepted February 6, 1979.

Maintaining Sparsity In Process Design Calculations

MARK A. STADTHERR

Chemical Engineering Department
University of Illinois
Urbana, Illinois 61801

Sparse linear systems in bordered block-triangular form can be efficiently solved by block-triangular splitting, a new technique that provides a drastic reduction in the fill-in (loss of sparsity) that occurs in the direct solution of such systems. This technique is applicable in the iterative solution of the large systems of nonlinear equations that arise in the equation oriented approach to process simulation and design calculations.

SCOPE

In most programs for computer aided chemical process design, the computational work is organized into modules, each of which performs the computations for one sort of unit operation. In such programs, the computational modules are usually simulation oriented; that is, given the variables describing the input streams and the equipment, they calculate the variables describing the output streams. However, if a design problem is to be solved, it may be necessary to calculate an input variable or equipment parameter given an output variable. Design oriented modules can be provided, but because of the large number of possible design problems, an inordinately large number of such modules would have to be provided. In practice, a few design oriented modules are typically provided to handle the most common design problems. In other cases, the design problem must be solved by an iterative or controlled simulation, in which the process is repeatedly simulated until the desired values for the design variables are obtained. While this is reasonably effective for small processes of average complexity, it is much less so when applied to the design of the large, complex processes commonly found today.

In principle, this difficulty can be resolved by eliminating the computational modules and performing all computations simultaneously. The potential advantages of this global (or equation oriented) approach to the design problem are well recognized, but acceptance of this approach has been slow, primarily because of the difficulties involved in solving extremely large sets of nonlinear equations simultaneously. For solving such systems, Newton-Raphson or related techniques are typically most effective. These techniques require the periodic solution of a set of linear equations, which in this case will be extremely large and sparse. In solving large, sparse linear systems, a major difficulty is the loss of sparsity that occurs when the conventional elimination techniques are used. This fill-in may lead to excessive storage requirements and unacceptably long computational times. Thus, the acceptance of the global approach to computer aided chemical process design depends to a great extent on the development of efficient techniques for maintaining sparsity. The work described here is directed largely at the development and application of such techniques.

0001-1541-79-2714-0609-$00.85.